Successive Orbital Ordering Transitions in $NaVO_2$

T. M. McQueen,[1] P. W. Stephens,[2] Q. Huang,[3] T. Klimczuk,[4,5] F. Ronning,[4] and R. J. Cava[1]

[1]*Department of Chemistry, Princeton University, Princeton, New Jersey 08544, USA*
[2]*Department of Physics and Astronomy, SUNY, Stony Brook, New York 11794, USA*
[3]*NIST Center for Neutron Research, Gaithersburg, Maryland 20899, USA*
[4]*Condensed Matter and Thermal Physics, Los Alamos National Laboratory, Los Alamos, New Mexico 87545, USA*
[5]*Faculty of Applied Physics and Mathematics, Gdansk University of Technology, Narutowicza 11/12, 80-952 Gdansk, Poland*

(Received 2 May 2008; published 13 October 2008)

Physical property measurements on samples of triangular-lattice $NaVO_2$ reveal two successive orbital ordering transitions. At 300 K, the structure is rhombohedral. At 98 K, the system undergoes a second-order transition to a monoclinic phase in which the in-plane V-V distances separate into four short and two long bonds, corresponding to orbital ordering of one electron per V^{3+}. Below 93 K, there is a first-order transition to a second monoclinic phase with four long and two short V-V bonds, consistent with orbital ordering of two electrons per V^{3+}. Long range magnetic ordering of $0.98(2)\mu_B$ per V^{3+} ($3d^2$) sets in at the 93 K structural transition. The orbital ordering relieves the geometric frustration and leads to a magnetically ordered ground state.

DOI: 10.1103/PhysRevLett.101.166402 PACS numbers: 71.70.Gm, 75.25.+z, 75.30.Et, 75.50.Ee

Layered, triangular-lattice transition metal compounds exhibit a wide variety of magnetic and electrical properties [1–4]. The origin of these phenomena is often attributed to the frustrating geometry of the triangular lattice, which prevents all nearest-neighbor antiferromagnetic (AFM) interactions from being satisfied simultaneously and results in a highly degenerate ground state. Consequently, these systems often adopt low-temperature structures in which a distortion removes the degeneracy, favors a particular ground state, and lowers the total energy of the system. Orbital ordering (OO) has been suggested [5] as one mechanism by which the geometric frustration can be removed to lower the energy of the system. Both $NaTiO_2$ and $LiVO_2$ have been proposed [5] as systems that display this type of OO. However, there is controversy regarding the exact nature of the observed transition in $NaTiO_2$ [6,7], and the OO in $LiVO_2$ has only been inferred from superreflections, consistent with vanadium trimerization, in electron diffraction images of the low-temperature phase [8,9]. In this Letter, we report the presence of successive OO transitions in $NaVO_2$ with the low-temperature phase possessing long range magnetic order. This is in sharp contrast to $LiVO_2$, which undergoes a single transition to a nonmagnetic low-temperature phase. The observed orbital orderings in $NaVO_2$ are consistent with theoretical predictions [5] but different than that in $LiVO_2$. These results, when combined with prior work on $LiVO_2$ and $NaTiO_2$, suggest that a unified picture, based on removing unfavorable magnetic interactions by OO, explains the observed behavior in all of these compounds.

$NaVO_2$ has been previously studied [10,11], but, due to the rigorous synthetic and handling conditions required for this compound, the samples employed were poor and led to inaccurate deductions about its physical properties. We prepared the phase-pure high quality $NaVO_2$ used in this study as follows: Na_2CO_3 and V_2O_3 in the ratio 1.02:1 were intimately mixed and placed as a loose powder in a silver boat. The boat was heated quickly under a fast flow of $5\%H_2/95\%Ar$ gas in a quartz tube to 400 °C. The temperature was then slowly increased to 600 °C over 5 h and soaked for 7 h. The tube was then closed off to the gas flow (and air) and pumped directly into a glovebox. All further manipulations were carried out under strict oxygen and moisture-free conditions. The stoichiometry of the material used in this study was confirmed in three ways: free refinement of the Na:O ratio with the neutron diffraction data gave 0.99(1):2, refinement of the synchrotron x-ray data gave an Na:V ratio of 0.997(3):1, and inductively coupled plasma–optical emission spectroscopy analysis gave a Na:V ratio of 0.95(3):1. Within error, all three of these are consistent with the stoichiometric formula $NaVO_2$. $NaScO_2$, used to account for the lattice contribution to the specific heat, was prepared by mixing Na_2CO_3 and Sc_2O_3 powders in the ratio 1.02:1, pressing into a pellet, and heating at 700 °C for two days. High resolution x-ray powder diffraction (HRXRD) data were collected on the SUNY X16C beam line at the National Synchrotron Light Source. Power neutron diffraction (PND) patterns were taken at the NIST center for neutron research using the BT-1 and BT-7 powder diffractometers. Refinements of the PND and HRXRD were performed using GSAS with EXPGUI [12,13]. The composition was fixed at 1:1:2 for the final refinements. Magnetization, resistivity, and specific heat measurements on polycrystalline pellets were performed in a Quantum Design physical property measurement system.

The room temperature (HT) structure of $NaVO_2$ is rhombohedral, $R\text{-}3m$, and consists of 2D triangular-lattice VO_2 layers of edge sharing VO_6 octahedra separated by sodium ions, as shown in Fig. 1(b). Adjacent VO_2 layers

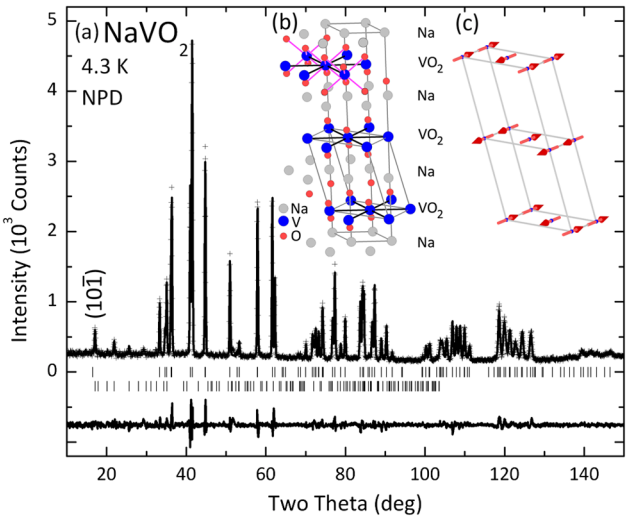

FIG. 1 (color online). (a) Fit of PND data at 4.3 K including both structural (upper ticks) and magnetic (lower ticks) components. (b) The structure of $NaVO_2$, showing the corner-sharing VO_6 octahedra within each VO_2 layer that form a triangular lattice, as well as *ABC*-type stacking to produce the full structure. The rhombohedral (hexagonal setting) and monoclinic unit cells used to describe the structure are also drawn. (c) The observed magnetic ordering in LT-$NaVO_2$.

are offset laterally with an *ABCABC*-type stacking to create a three-layer structure. Since the interlayer V-V spacing (~5.6 Å) is much greater than the intralayer one (~3.0 Å), the system is expected to act in a pseudo-2D manner. In the HT phase, all six in-plane nearest-neighbor V-V bond distances are crystallographically equivalent. Above $T = 98$ K, $NaVO_2$ has this ideal HT structure, and, as shown in Fig. 2(a), the V-V distance is 2.9959(2) Å at 100 K. On cooling below $T = 98$ K, the system undergoes a continuous phase transition to a monoclinic, $C2/m$, intermediate temperature (IT) phase that has two long and four short V-V distances. At the point of maximal distortion $T = 93$ K, the distances are 3.0050(4) (two) and 2.9866(2) Å (four). The second-order nature of this transition is shown through the gradual splitting of the rhombohedral (211) reflection [Fig. 2(a) (inset)]. With further cooling, the system undergoes a discontinuous phase transition to the low-temperature (LT) phase, which is also monoclinic but has four long and two short distances, 2.9770(4) Å (two) and 3.0146(6) Å (four). These bond lengths are similar to the maximum values in the IT phase, but with the long and short bonds reversed. Unlike the HT to IT transition, the transition between the IT and LT phases is first-order: When the temperature is lowered, the pair of peaks corresponding to the IT phase decrease in intensity but do not shift positions when the peaks corresponding to the LT phase appear and increase in intensity [Fig. 2(a) (inset)]; thus a two-phase region separates the LT and IT phases, indicative of a first-order phase transition.

The observed magnetic properties of $NaVO_2$ track these structural changes. As shown in Fig. 2(b), the magnetic susceptibility drops significantly as the IT phase develops, from $20.2(2) \times 10^{-4}$ emu/mol at 100 K to $19.2(2) \times 10^{-4}$ emu/mol. There is only a small decrease in susceptibility at the IT to LT transition at $T = 93$ K. However, the fraction of magnetic moments that are long range ordered, extracted from the magnetic (10$\bar{1}$) peak in the PND data that arises solely from magnetic scattering, stays near zero during the transformation from the HT to IT phase. It then increases in value as the LT phase develops, as shown in Fig. 2(c). Thus we associate the decrease in magnetic susceptibility at $T = 98$ K with the HT to IT transition and the formation of long range 3D magnetic order $T = 93$ K with the IT to LT transformation.

There were no observable changes in the PND data between 80 and 1.8 K, so PND data suitable for magnetic structure refinement were collected at 4.3 K. The magnetic reflections were indexable with the LT unit cell but with a doubled c axis. The most intense magnetic reflection is (10$\bar{1}$), and so the moments were taken to align with the b axis. The final refinement is shown in Fig. 1(a), and the refined magnetic structure is shown in Fig. 1(c). Within each layer of vanadium ions, a magnetic moment of $0.98(2)\mu_B$ per V^{3+} is observed to lie along the direction of the short V-V bond distance forming ferromagnetic

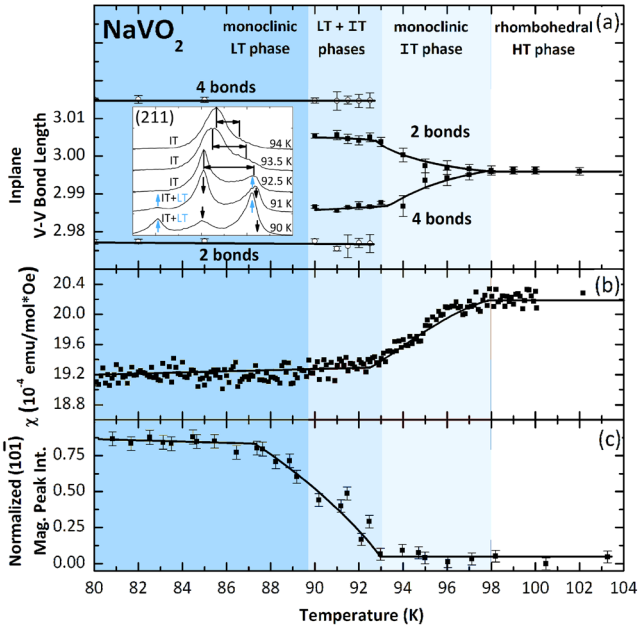

FIG. 2 (color online). (a) In-plane V-V bond distances, as determined by unit cell refinements of HRXRD data. Inset: X-ray scans of the rhombohedral (211) reflection, showing a continuous splitting of the peak transitioning from the HT to IT phase, followed by a two-phase region of the IT and LT forms. (b) Magnetic susceptibility, corrected for the sample holder and diamagnetism of core electrons. (c) The fraction of the 3D ordered magnetic phase present, as determined by the intensity of the (10$\bar{1}$) magnetic-only reflection from PND data.

chains; adjacent chains are aligned antiferromagnetically with respect to each other. These planes are stacked so that nearest-neighbor chains between layers are also aligned antiferromagnetically.

The refined magnetic moment per site in the ordered phase is half the expected value: $gS = 2\mu_B$. A Curie-Weiss fit of the high temperature susceptibility [see Fig. 3(a)] is consistent with a p_{eff} of either 1.87 ($J = 1/2$) or 2.86 ($J = 1$). However, for both fits the magnitude of the Weiss temperature is greater than 320 K, implying that the fits for the temperature range of the measurement, and hence the effective moments, are not reliable. To get at the moment per V^{3+}, we instead extracted the value of J from fits of the $M(H)$ curves to the Curie law [14] [Fig. 3(b) (inset)], which approaches the value of $J \sim 1/2$ [Fig. 3(b)]. This limit is consistent with the observed moment of $0.98(2)\mu_B$. Integration of the specific heat data, where the lattice contribution has been removed by subtraction of the scaled data on isostructural $NaScO_2$ [Fig. 3 (inset)], shows that the entropy recovered on heating from 1.8 to 300 K is slightly larger than $R\ln(2)$ [Fig. 3(c)]. This entropy change is consistent with a two-level magnetic system, where the residual entropy above $R\ln(2)$ comes from the observed structural and orbital changes. Thus we conclude that each V^{3+} site behaves as though it is $J = 1/2$, rather than the expected $J = 1$. This reduced magnetic moment is surprising as $NaVO_2$ is insulating, even in the HT phase, suggesting localized electronic behavior. The resistivity data on a polycrystalline pellet are shown in Fig. 3(a) (inset); the band gap of HT $NaVO_2$ is estimated to be 0.27(1) eV.

These structural and magnetic properties of $NaVO_2$ are consistent with two successive orbital orderings. In the HT phase, the V^{3+} coordination environment is nearly octahedral, and thus we expect the bands derived from the $3d$ orbitals to be split into a lower T_{2g} and upper E_g set. Because of the $\bar{3}m$ symmetry, the T_{2g} manifold is further split into a singly degenerate A_1 band and a doubly degenerate E band [Fig. 4(a) (i)]. Since the $\bar{3}m$ splitting is known to be small in related compounds, such as $LiVO_2$, at high temperatures we expect the two valence electrons to equally occupy all three states. As the temperature is lowered, we expect the occupancy of the A_1 band to increase at the expense of the E band. Initially, this would not cause any structural change as the orbital lobes of the A_1 band on a V^{3+} cation point equally toward all six in-plane nearest-neighbor V^{3+} sites, although deviations from ideal behavior in the magnetic susceptibility and specific heat would still be expected. Both of these are observed: Although HRXRD shows no observable structural distortion until $T = 98$ K, the data presented in Fig. 3 suggest that the properties of $NaVO_2$ are changing at much higher temperatures, starting at $T \approx 230$ K. However, this in-

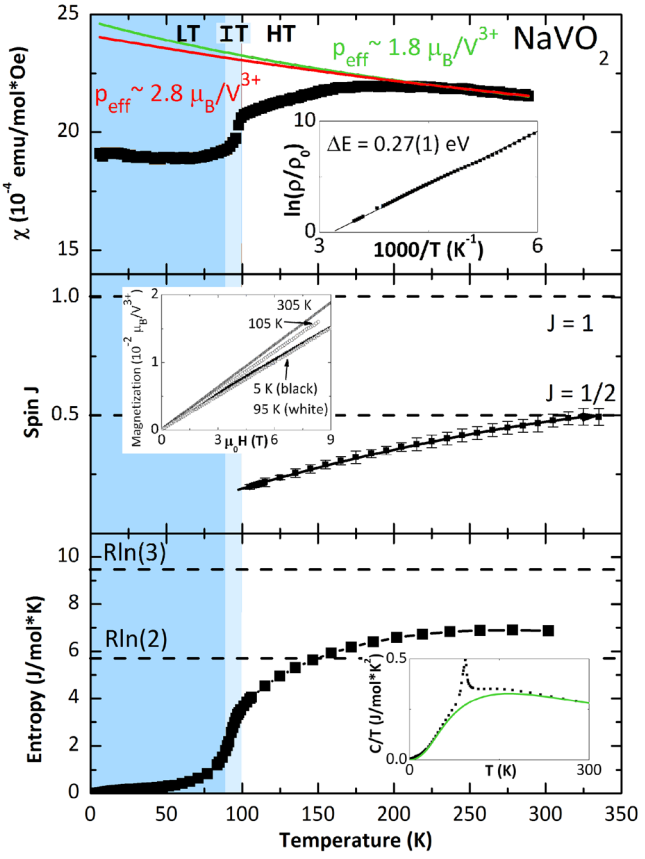

FIG. 3 (color online). (a) Magnetic susceptibility of $NaVO_2$ from 5 to 300 K. The data are consistent with either one or two magnetic spins per V^{3+}. Inset: Scaled resistivity from a polycrystalline pellet shows that even the HT phase is insulating. (b) Fits of $M(H)$ curves (drawn in the inset) to the Curie law suggest that there is one magnetic electron per V^{3+}. (c) Integration of the raw specific heat data (drawn in the inset), with the lattice contribution removed by subtraction of scaled $NaScO_2$ data, integrates to a value slightly higher than $R\ln(2)$, suggesting a two-level magnetic system.

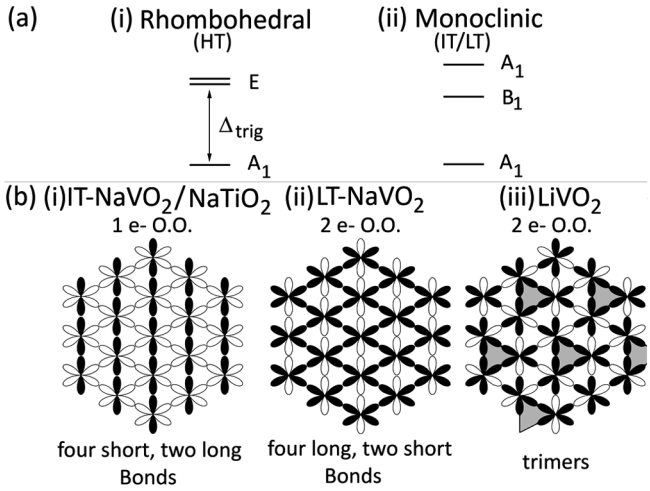

FIG. 4. (a) Proposed, simplified band picture for $NaVO_2$-type materials in the (i) HT (rhombohedral) and (ii) LT (monoclinic) structures. (b) Proposed orbital orderings in (i) IT-$NaVO_2$/$NaTiO_2$, (ii) LT-$NaVO_2$, and (iii) $LiVO_2$. Only the in-plane lobes are drawn; filled lobes are shaded in black. The resulting trimers in (iii) are lightly shaded.

creasing population of the A_1 band results in an increase in the geometric magnetic frustration since the orbitals point toward all six nearest neighbors, and simultaneously satisfying these AFM interactions is not possible. The system then undergoes a distortion that relieves the geometric frustration. In the IT phase, with four short and two long distances, the lower A_1 band is derived from orbitals whose in-plane components point toward two nearest neighbors, 180° apart. Thus the transition to the IT phase corresponds to the localization of one electron per site in the A_1 band, with the second electron equally occupying the two remaining degenerate E states. This is OO of one electron and is schematically drawn in Fig. 4(b) (i). The two V-V distances along the direction of the filled orbital increase in length compared to the HT phase, whereas the other four V-V distances decrease. This ordering, in addition to relieving the geometric frustration, splits the degeneracy of the E band into B_1 and upper A_1 levels [Fig. 4(a) (ii)]. The IT to LT transition then corresponds to population of the B_1 band (from the upper A_1 band) to form a fully OO state, as shown in Fig. 4(b) (ii). Compared to the IT phase, this LT phase has four bonds that are longer (the directions in which the occupied orbitals lie) and two that are shorter (the direction of the unoccupied orbitals). Thus $NaVO_2$ exhibits two successive OO transitions, corresponding to OO of each of the two electrons per site. The observed arrangement of spins in the LT phase is consistent with the proposed OO. Empty orbitals lie along the two short V-V bond axes, which would favor ferromagnetic exchange between adjacent sites along the chains, whereas the filled orbitals lie along the four long V-V bond axes between chains, which would favor AFM interactions between chains. The magnetic structure of LT-$NaVO_2$ has this exact arrangement.

This picture also explains the observed behavior in $NaTiO_2$. The distortion exhibited by IT-$NaVO_2$ [Fig. 4(b) (i)] is analogous to the one reported [6] for $NaTiO_2$, with four short and two long in-plane bond distances. When $NaTiO_2$ undergoes the distortion to the low-temperature monoclinic phase, the geometric frustration is relieved, just as in the case of IT-$NaVO_2$, by transitioning to a structure where the lower A_1 band points principally to only two nearest neighbors, rather than all six. This explanation holds whether the one valence electron in the high temperature rhombohedral phase of $NaTiO_2$ is orbitally polarized (only in the A_1 band) or not (spread out over A_1 and E bands), i.e., whether or not there is a change in the orbital occupancies through the transition. In contrast, despite having the same structure and electron count as $NaVO_2$, the observed structural changes [8] in $LiVO_2$ appear to be very different: The low-temperature structure is pseudorhombohedral with no observed long range magnetic ordering.

Previous theoretical work [5] has suggested that there are two possible OO schemes for two electrons on a triangular lattice: the ordering observed in LT-$NaVO_2$ [Fig. 4(b) (ii)] or the alternate arrangement, proposed for $LiVO_2$ [Fig. 4(b) (iii)]. In this latter case, the OO results in the formation of nonmagnetic vanadium trimers (shaded regions). Our data suggest that, in $LiVO_2$, the trimer state is stabilized relative to the LT-$NaVO_2$ ordering scheme by a further lattice distortion that increases d-d hybridization. In $NaVO_2$, this further stabilization is not possible, due to the larger size of the lattice compared to $LiVO_2$. This hypothesis is supported by the fact that in $LiVO_2$ the average in-plane V-V distance through the transition shrinks from 2.91 to 2.84 Å [8], indicating a significant increase in metal-metal bonding, whereas in $NaVO_2$ the mean bond length is longer, near 3.00 Å, and stays relatively unchanged through the OO transitions. We conclude that the temperature-dependent properties of $NaVO_2$ can be explained in terms of OO and geometric magnetic frustration. We find that the magnetic structure in LT-$NaVO_2$ refines to only $0.98(2)\mu_B/V^{3+}$, despite having two electrons per site. Since $NaTiO_2$ is not reported to show an ordered magnetic state above or below its transition [6], we propose that one electron in $NaVO_2$ acts in the same manner as the one electron per Ti site in $NaTiO_2$, and thus it is only the second electron that is responsible for the magnetic characteristics. Further studies would be of interest to elucidate the origin of this observed behavior.

T. M. M. gratefully acknowledges support of the National Science Foundation Graduate Research Fellowship Program. This work was done under NSF DMF Grant No. NSF-DMR-0703095. Use of the National Synchrotron Light Source, Brookhaven National Laboratory, was supported by the U.S. Department of Energy, Office of Science, Office of Basic Energy Sciences, under Contract No. DE-AC02-98CH10886.

[1] K. Takada *et al.*, Nature (London) **422**, 53 (2003).
[2] R. E. Schaak *et al.*, Nature (London) **424**, 527 (2003).
[3] M. L. Foo *et al.*, Solid State Commun. **133**, 407 (2005).
[4] A. Olariu *et al.*, Phys. Rev. Lett. **97**, 167203 (2006).
[5] H. F. Pen *et al.*, Phys. Rev. Lett. **78**, 1323 (1997).
[6] S. J. Clarke *et al.*, Chem. Mater. **10**, 372 (1998).
[7] S. Y. Ezhov *et al.*, Europhys. Lett. **44**, 491 (1998).
[8] W. Tian *et al.*, Mater. Res. Bull. **39**, 1319 (2004).
[9] K. Imai *et al.*, J. Solid State Chem. **114**, 184 (1995).
[10] M. Onoda, J. Phys. Condens. Matter **20**, 145205 (2008).
[11] B. L. Chamberland and S. K. Porter, J. Solid State Chem. **73**, 398 (1988).
[12] A. C. Larson and R. B. Von Dreele, Los Alamos National Laboratory Report LAUR 86, 2000.
[13] B. H. Toby, J. Appl. Crystallogr. **34**, 210 (2001).
[14] N. W. Ashcroft and N. D. Mermin, *Solid State Physics* (Brooks/Cole, Ithaca, 1976).